



Comparison of N-linked glycosylation on hemagglutinins derived from chicken embryos and MDCK cells: a case of the production of a trivalent seasonal influenza vaccine

Jingqi Li¹ · Sixu Liu¹ · Yanlin Gao^{1,2} · Shuaishuai Tian¹ · Yu Yang³ · Ningning Ma¹

Received: 20 November 2020 / Revised: 11 March 2021 / Accepted: 16 March 2021 / Published online: 3 May 2021
© The Author(s), under exclusive licence to Springer-Verlag GmbH Germany, part of Springer Nature 2021

Abstract

N-linked glycosylation plays critical roles in folding, receptor binding, and immunomodulating of hemagglutinin (HA), the main antigen in influenza vaccines. Chicken embryos are the predominant production host for influenza vaccines, but Madin-Darby canine kidney (MDCK) cells have emerged as an important alternative host. In this study, we compared glycosylation patterns, including the occupancy of potential glycosylation sites and the distribution of different glycans, on the HAs of three strains of influenza viruses for the production a trivalent seasonal flu vaccine for the 2015–2016 Northern Hemisphere season (i.e., A/California/7/2009 (H1N1) X179A, A/Switzerland/9715293/2013 (H3N2) NIB-88, and B/Brisbane/60/2008 NYMC BX-35###). Of the 8, 12, and 11 potential glycosylation sites on the HAs of H1N1, H3N2, and B strains, respectively, most were highly occupied. For the H3N2 and B strains, MDCK-derived HAs contained more sites being partially occupied (<95%) than embryo-derived HAs. A highly sensitive glycan assay was developed where 50 different glycans were identified, which was more than what has been reported previously, and their relative abundance was quantified. In general, MDCK-derived HAs contain more glycans of higher molecular weight. High-mannose species account for the most abundant group of glycans, but at a lower level as compared to those reported in previous studies, presumably due to that lower abundance, complex structure glycans were accounted for in this study. The different glycosylation patterns between MDCK- and chicken embryo-derived HAs may help elucidate the role of glycosylation on the function of influenza vaccines.

Key points

- For the H3N2 and B strains, MDCK-derived HAs contained more partially (<95%) occupied glycosylation sites.
- MDCK-derived HAs contained more glycans of higher molecular weight.
- A systematic comparison of glycosylation on HAs used for trivalent seasonal flu vaccines was conducted.

Keywords Influenza vaccine · Hemagglutinin · *N*-linked glycosylation · Glycan occupancy · Madin-Darby canine kidney (MDCK) cells

✉ Yu Yang
yangyu@syphu.edu.cn

✉ Ningning Ma
maningning@syphu.edu.cn

¹ Wuya College of Innovation, Shenyang Pharmaceutical University, Wenhua Road 103, Shenyang 110016, Liaoning Province, China

² Present address: School of Computing, Urban Sciences Building, Newcastle University, 1 Science Square, Newcastle Helix, Newcastle upon Tyne NE4 5TG, UK

³ School of Life Science and Biopharmaceutics, Shenyang Pharmaceutical University, Wenhua Road 103, Shenyang 110016, Liaoning Province, China

Introduction

Hemagglutinin (HA), the dominant antigen in influenza vaccines, is a glycoprotein with multiple *N*-linked glycans. Glycosylation is critical for the function and immunogenicity of HAs. Firstly, glycans on the HA stem region participate in the folding of HAs by recruiting lectin chaperones to facilitate the folding process (Hebert et al. 1997; Daniels et al. 2003). Secondly, glycosylation increases the hydrophilicity of HAs, which reduces aggregation during the intracellular transportation of HAs (Roberts et al. 1993; Gallagher et al. 1992). Thirdly, glycans, especially those in the vicinity of receptor binding site (RBS), can modulate virus receptor binding. The

addition of a glycosylation site to the HAs of A/Aichi/2/68 (H3N2) via genetic engineering reduced its ability to bind to guinea pig and chicken erythrocytes (Abe et al. 2004). A similar phenomenon was observed for a A/Hong Kong/1/68 (H3N2) strain (Alymova et al. 2016). Fourthly, glycans may alter the immunogenicity of HA proteins. Glycans could mask underlying antigenic epitopes, thereby enabling influenza viruses to evade recognition and neutralization by the immune system (Abe et al. 2004; Hütter et al. 2013; Skehel et al. 1984; Wrigley et al. 1983; Das et al. 2011; Wei et al. 2010; Medina et al. 2013; Matrosovich et al. 1999; Wang et al. 2010; Ohuchi et al. 1997). Evolutionary studies of influenza A virus subtypes H1N1 and H3N2 indicate that under immune pressure, the number of glycosylation sites on the HA globular head unremittingly increases over time (Sun et al. 2011; Blackburne et al. 2008; Zhang et al. 2004; Cherry et al. 2009; Kobayashi and Suzuki 2012).

Embryonated hen eggs have been used for influenza vaccine production for over 70 years (Gerdil 2003). Cell culture-based production processes had gained great attention in addressing the various limitations of embryo-based processes, such as long lead time for supply, high contamination risks due to multiple open steps, and potential mutations on HAs during embryo adaptations. Three cell lines, Vero, Madin-Darby canine kidney (MDCK), and EB66, have been approved for inactivated seasonal or pandemic influenza vaccine production (Pérez Rubio and Eiros 2018, <https://www.pmda.go.jp/files/000229076.pdf>, <https://www.pmda.go.jp/files/000229077.pdf>). There are only two seasonal influenza vaccines based on cell culture, Flucelvax® and SKYCellflu®, which are on the market and both vaccines are produced by MDCK cells (Rockman et al. 2020). In 2016, Flucelvax® became the first approved flu vaccine to use MDCK cell-isolated viral seeds instead of embryo-isolated seeds. One key advantage of the MDCK cell line is its universality for the efficient propagation of a wide range of influenza strains (Pérez Rubio and Eiros 2018; Kaiser 2006). This quality is desirable in a platform production process, where only a very tight timeframe is available for process adaptation between the annual strain nomination and vaccine production. Other advantages of cell culture-based processes include short lead time and low risk of contamination.

Patterns of *N*-linked glycosylation, including glycan structures and glycosylation site occupancy, are highly reliant on production hosts. Schwarzer et al. (2009) compared glycosylation patterns of HAs of three influenza strains, H1N1, H3N2, and B, that were produced in six different cell lines, including two canine (a MDCK and a mutated MDCK), one monkey (Vero), one avian (AGE.1), and two human (A549 and HepG2). Glycoforms were analyzed with a capillary gel electrophoresis with laser-induced fluorescence detection (CGE-LIF) assay. Host cells were found to have a profound impact on glycosylation patterns, including the number

of glycan peaks and relative heights of the peaks. Yagi et al. (2012) compared glycosylation structures of HAs of an H3N2 strain derived from MDCK and an embryo using high-performance liquid chromatography (HPLC) glycan mapping and matrix-assisted laser desorption/ionization-time-of-flight mass spectrometry (MALDI-TOF-MS) assays. Around 29 glycoforms were identified, and significant variation in abundance was observed. MDCK-derived HAs contained less sulfated glycans, but more high-mannose glycans. Recently, An et al. (2019) studied glycosylation of the reference antigens of a trivalent vaccine for the 2014–2015 influenza season that were produced in chicken embryos, MDCK cells, or insect cells (Sf9). The authors quantified the overall distributions of glycans, as well as the distribution of glycans at specific glycosylation sites, using mass spectrometry-based analytical assays. The number of glycans identified for each sample was between 13 and 29. It is concluded that the glycan distribution was dependent on both the virus and the production host. HAs derived from Sf9 cells contain mostly pauci-mannose structures. H1N1 antigens, including both HAs and neuraminidases (NAs), derived from MDCK cells contain more high-mannose species than chicken embryo-derived antigens, but the opposite was true for B antigens in that chicken embryo-derived antigens contain more high-mannose species. The most dominant glycan on different glycosylation sites also showed a dramatic difference between MDCK and chicken embryo-derived antigens (a mixture of HAs and NAs) for all three strains.

The systematic comparison of glycosylation patterns between HA-derived from chicken embryo and MDCK cells is still limited. Yagi et al. (2012) investigated only a single strain (H3N2) for glycan distribution differences between an embryo and MDCK cell-derived viruses. An et al. (2019) studied glycosylation of antigens in a trivalent vaccine derived from embryos and MDCK cells, but the antigens were mixtures of HA and NA proteins when the released glycans were analyzed. The occupancy of potential glycosylation sites is equally as important as glycan distribution. Zhang et al. (2012) studied recombinant HAs of A/California/04/09 (H1N1) produced in both plant and insect cells and found that two potential glycosylation sites were partially occupied (50–80%) in both cases. An et al. (2015) found that for an engineered H3N2 strain produced in MDCK cells, 9 of the 11 potential sites on HAs had an occupancy higher than 90% while the remaining two sites were undetermined. A systematic comparison of glycosylation occupancy on HAs derived from embryos and MDCK cells for trivalent or quadrivalent vaccines is still needed.

In this study, we compared the distribution of different glycans and site occupancy of purified HAs derived from chicken embryos and MDCK cells. Three influenza strains were investigated, A/California/7/2009 (H1N1) X179A, A/Switzerland/9715293/2013 (H3N2) NIB-88, and

B/Brisbane/60/2008 NYMC BX-35###, which were nominated for the trivalent seasonal flu vaccine for the 2015–2016 Northern Hemisphere season. This is the first systematic comparison of glycosylation patterns conducted on purified HA proteins produced by two of the most important hosts for influenza vaccine production.

Materials and methods

Virus seed and propagation

Three influenza vaccine strains were used, which were kindly provided by the Wuhan Institute of Biological Products, China. The three strains were recommended for the production of trivalent seasonal influenza vaccines for use in the 2015–2016 Northern Hemisphere season, including A/California/7/2009 (H1N1) X179A, A/Switzerland/9715293/2013 (H3N2) NIB-88, and B/Brisbane/60/2008 NYMC BX-35###, subsequently referred to as X179A (H1N1), NIB-88 (H3N2) and BX-35### (B) for simplicity. All three strains were propagated in chicken embryos and MDCK cells, but only the embryo-derived viruses were used as seed viruses.

Standard procedures were used to propagate the influenza virus in chicken embryos. Briefly, nine-day-old chicken embryos (Beijing Boehringer Ingelheim Vital Biotechnology, China) were infected and incubated at 33 °C and 60% humidity for 48 h and then at 4 °C overnight. Allantoic fluid was harvested, inactivated with 0.125% β -propiolactone (Macklin, China) overnight at 37 °C, 0.2 μ m filtered, and stored at 4 °C.

MDCK-derived influenza viruses were produced with a clonal MDCK cell line that was developed in house from the parental MDCK CCL-34 cell line (ATCC, US). The clonal MDCK cell line had been adapted for serum-free and suspension cultures. MDCK cells were routinely maintained in serum-free MDCK 302 medium (Vbiosci, China) at a seeding density of 0.5×10^6 cells/mL and subcultured every 3 d. For vaccine production, MDCK cells were cultured in a 1:1 combination of serum-free MDCK 302 and serum-free MDCK 303 medium (Vbiosci, China) in either 250 mL shake flasks (Corning, US) or 3 L bioreactors (Eppendorf, US). When cell viability dropped below 50%, cell culture supernatant was harvested, and viral particles were inactivated with 0.125% β -propiolactone overnight at 37 °C, 0.2 μ m filtered, and stored at 4 °C.

HA sequencing

Standard reverse transcription-polymerase chain reaction (RT-PCR) and sequencing protocols were followed. Forward and reverse transcription primers were designed

based on respective HA sequences found on the Global Initiative on Sharing All Influenza Data (GISAID) website. Forward primer 5'-ATGAAGGCAATACTAGTAGTT-3' and reverse primer 5'-TTAAATACATATTCTACTGTA-3' were used for X179A (H1N1); forward primer 5'-ATGAAGACTATCATTGCTTTGAGC-3' and reverse primer 5'-ATGCACTCAAATGCAAATGTTGC-3' were used for NIB-88 (H3N2); and forward primer 5'-ATGAAGGCAATAATTGTACT-3' and reverse primer 5'-TTATAGACAGATGGAGCATG-3' were used for BX-35### (B). The sequencing results have been deposited in GenBank (MW296843 for X179A (H1N1), MW300957 for NIB-88 (H3N2), and MW301041 for BX-35### (B)).

SDS-PAGE and WB

Sodium dodecyl sulfate-polyacrylamide gel electrophoresis (SDS-PAGE) and western blot (WB) were carried out under non-reducing conditions. For the WB assay, anti-HA-tag (MBL, M180-3) and goat anti-mouse IgG Fc (Thermo Fisher, #31439, US) antibodies were used as the primary and secondary antibodies, respectively.

Electron microscopy

Viral particles were stained with tungsten phosphate (Sigma, US) and observed under a transmission electron microscope (Hitachi, H7650, Japan).

Purification of virus particles

Viral particles in either allantoic fluid or cell culture supernatant were purified by sucrose concentration gradient ultracentrifugation. Briefly, samples were loaded on chilled 30% sucrose and centrifuged at $113,000 \times g$ (Beckman, SW28) for 2 h at 4 °C. The viral particle layer was resuspended in TNC buffer (pH 7.40, 1 M NaCl, 0.02 M Tris-HCl, 0.05 M CaCl_2), loaded on layers of 55%, 45%, and 35% sucrose solutions, and centrifuged at $230,000 \times g$ for 10 h at 4 °C (Beckman, SW60Ti). The viral particles in the target layer were then washed with TNC buffer and stored at -80 °C.

Purification of HA glycoproteins

A total of 180 μ g virus particles were loaded in SDS-PAGE to separate HA from other viral proteins. Gel strips containing the HA band were excised from the gel, and HAs were extracted in a buffer solution (pH 7.5, 0.1% SDS, 25 mM glycine, and 25 mM Tri-HCl) at 4 °C overnight. Gel components were spun down and HA glycoproteins in the supernatant was concentrated and washed with ultrafiltration tubes (Sartorius, VN01H02, Germany) to a final concentration of 0.5 mg/mL (in 100 μ L 50 mM NH_4HCO_3).

Determination of glycan occupancy

Purified HA protein was digested with peptide-N-glycosidase F (PNGase F; New England Biolab, #P0704S, US) to remove N-linked glycans. Glycan occupancy was determined by peptide mapping of deglycosylated HA. Multiple enzymes were used, including trypsin (Promega, VA1160, US), chymotrypsin (Sigma, US), or a combination of trypsin (Sigma, US) and Glu-C (Sigma, US). The digested mixtures were loaded on a 2.1 mm × 100 mm UltraPerformance CSH C18 column (Waters, US) on an HPLC (Shimadzu, Nexera X2 LC-30AD, Japan) and eluted into the electrospray ionization (ESI) source of a triple TOF mass spectrometer (AB, SCIEX 4600, US) with a 2–34 min gradient from 2 to 90% phase B (phase A: water with 0.1% formic acid; phase B: acetonitrile) at a constant flow rate of 0.25 mL/min. The electrospray voltage was at 5.5 kV. The normalized collision energy was at 10.0%. Liquid chromatography-mass spectrometry (LC-MS) spectra were collected by Analyst TF 1.7.1 (AB SCIEX, US) and mapped by Peakview 2.2 (AB SCIEX, US).

Quantification of the distribution of glycans

HAs were digested with PNGase F in 200 µL, after digestion, 600 µL of absolute ethanol was added, and the mixture was kept in -20 °C for 2 h before it was centrifuged at 13,000g for 30 min in 4 °C. The released N-glycans were free in the supernatant, while the deglycosylated proteins were in the precipitate. And glycans in the supernatant were dried in a vacuum centrifugal concentrator (Christ, RVC 2-18 CDplus, Germany), re-suspended in purified water, and fluorescently labeled with procainamide (PA) and 2-methylpyridine (2PB) in 30% acetic acid/dimethyl sulfoxide (DMSO). PA-labeled glycans were purified with LudgerClean S Cartridges (LC-S-A6, Ludger, UK). Glycans of different structures were separated with a hydrophilic chromatographic column (HILIC; Waters, X Bridge® Glycan BEH Amide 130 Å 3.5 µm 4.6 × 250 mm, US) on an HPLC (Shimadzu, Nexera X2 LC-30AD, Japan) equipped with a fluorescence detector (excitation wavelength 310 nm and emission wavelength 370 nm). Mobile phase A was 50 mM ammonium formate, and mobile phase B was 100% acetonitrile. The eluent was analyzed with a mass spectrometer (AB, SCIEX Triple TOF 4600, US), and glycan structures were determined by GlycoWorkbench based on both primary and secondary mass spectra.

For enzymatic cleavage of glycans, PA-labeled glycans were digested with endoglycosidase H (Endo H_f) (New England Biolab, #P0703S, US) or α1-2,3,6 mannosidase (New England Biolab, #P0768S, US) at 37 °C overnight and inactivated at 95 °C for 10 min.

Results

Production and purification of HA proteins

Three strains of influenza viruses were propagated in both chicken embryos and MDCK cells. Seeding viruses were derived from chicken embryos. The HAs of viruses propagated in either host was purified and analyzed similarly, as shown in Fig. 1a.

First, viral particles in either allantoic fluid or cell culture medium were separated from tissue or cellular contaminants by sucrose concentration gradient ultracentrifugation. Viral particles were split in the SDS-PAGE loading buffer, and HA proteins were separated from other viral proteins by non-reducing SDS-PAGE. HA proteins were extracted from SDS-PAGE gel strips and digested with PNGase F to cleave N-linked glycans from HAs. The released glycans were purified, fluorescently labeled, and analyzed to determine glycan structures and corresponding abundances. The deglycosylated HAs were analyzed by peptide mapping to determine the occupancy of the potential glycosylation sites.

After sucrose gradient density ultracentrifugation, a milk-white band of viral particles was visible at about 50% sucrose (Fig. 1b), and viral particles inside the bands were confirmed under electron microscopy (Fig. 1c). Non-reducing SDS-PAGE was able to separate HA from other viral proteins, as seen in Fig. 1d. Companion WB assays were used to identify the HA bands (Fig. 1e).

HA sequencing and analysis of potential glycosylation sites

HAs of all three strains propagated by both chicken embryos and MDCK cells were sequenced. For each strain, there was no sequence variation observed between the embryo and MDCK-derived HAs. Nucleic acid and amino acid sequences for all three strains are listed in Fig. S1 and Fig. 2a–c, respectively.

Structures of HA monomers of all three strains presented in Fig. 2a–c were modeled by PyMOL (<https://www.pymol.org/>) based on existing protein frameworks (Zhang et al. 2010; Dreyfus et al. 2012; Lee et al. 2014). The PDB files and Influenza virus strains used for modeling HAs structures were 3AL4, Influenza A virus (A/California/04/2009(H1N1)), 4O5N, Influenza A virus (A/Singapore/H2011.447/2011(H3N2)), 4FQM, Influenza B virus (B/Brisbane/60/2008) respectively. There were 8, 12, and 11 potential N-linked glycosylation sites for the H1N1, H3N2, and B strains, respectively, as labeled in Fig. 2a–c. The majority of the sites, 6 of 8, 11 of 12, and 7 of 11, were located in the HA1 region for X179A (H1N1), NIB-88 (H3N2), and BX-35### (B) respectively. It should be noted that X179A (H1N1) had no potential glycosylation site close to the receptor-binding

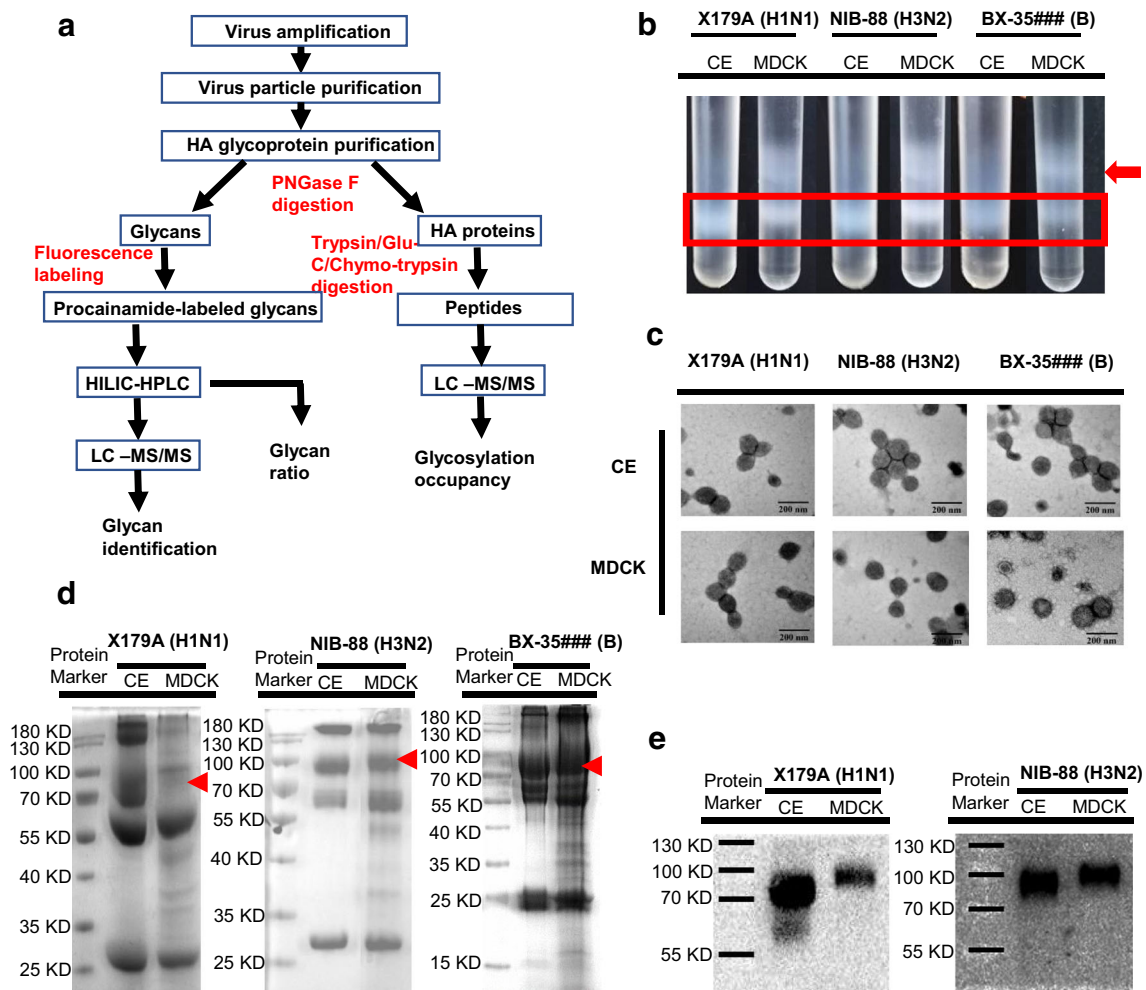


Fig. 1 Overall analytical strategy (**a**) and purification of virus particles and HA proteins. Bands of viral particles (shown in the box) after sucrose gradient density centrifugation (**b**) and viral particles observed under an

electron microscope at $\times 200,000$ (**c**). HA bands in non-reducing SDS-PAGE indicated by arrows (**d**) and the corresponding WB (**e**). CE, chicken embryo-derived HAs; MDCK, MDCK-derived HAs

region, while NIB-88 (H3N2) and BX-35### (B) have 5 and 4 respectively.

Occupancy of potential glycosylation sites

Site occupancy at each potential glycosylation site was determined by peptide mapping. The occupancy ratio at each specific site is defined by the ratio of asparagine (Asn) being converted to aspartic acid (Asp) post-PNGase F cleavage. Peptides of deglycosylated HA were generated primarily by trypsin digestion, but digestion by chymotrypsin or a combination of trypsin and Glu-C was also used in order to broaden site coverage. Table S1 summarizes the theoretical sequences of peptides that contain potential glycosylation sites. Theoretical and observed mass-charge values (m/z) of both occupied and unoccupied isoforms were also included. Theoretical m/z of primary spectrometry was used to identify target peptides, and fragment information of secondary mass spectrometry was used to verify the sequence of the peptides

(one example is shown in Fig. S2). The delta between theoretical and observed mass-charge values and the abundance (peak area) of the ionized peptides were also shown in Table S1.

Results of overall site occupancy are summarized in Table 1. There were three potential glycosylation sites missing, including two on the HAs of X179A (H1N1) and one on the HAs of BX-35### (B), as the corresponding peptides could not be recovered post-digestion. Other than the three undetermined sites, most potential sites were either completely or nearly completely ($>95\%$) occupied. Where sufficient signal was available, there were no sites that were completely unoccupied.

The number of partially occupied glycosylation sites and the occupancy levels differed between HAs derived from chicken embryos and MDCK cells for the H3N2 and B strains. For H3N2, there are three sites (#4, #6, and #8) that are at low occupancy (54.8% or lower) for both embryo and MDCK-derived HAs, and for all three sites, the occupancy

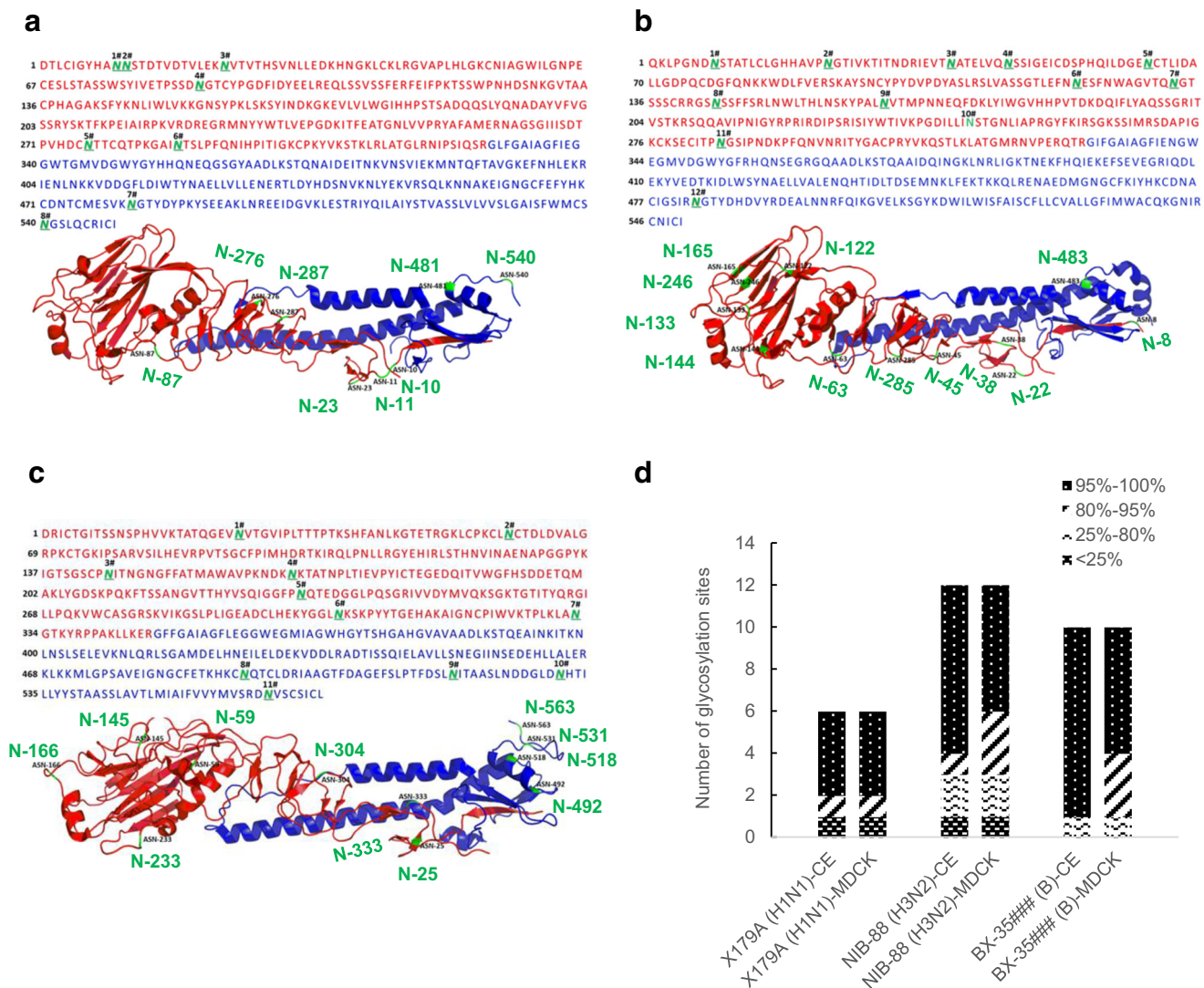


Fig. 2 Potential glycosylation sites on HAs of **a** X179A (H1N1), **b** NIB-88 (H3N2), and **c** BX-35### (B), as well as the distribution of measured site occupancy (**d**). Predicted glycosylation sites were labeled (green font)

level was lower in MDCK-derived HAs than in embryo-derived HAs. In addition, MDCK-derived H3N2 HAs had three more sites (#1, #2, and #10) that were partially occupied (88.2–94.5%), while the corresponding sites on embryo-derived HAs were all more than 94.5% occupied and two sites (#1 and #2) were even close to fully occupied (>95%). Overall occupancy on HAs of embryo-derived B strain was also higher than that of MDCK-derived B strain. Both MDCK- and embryo-derived B strain HAs had one site (#11) of low occupancy. However, MDCK-derived HAs had two more sites (#2 and #8) that were partially occupied (87.7% and 84.4%, respectively), while the corresponding sites on embryo-derived HAs were nearly completely occupied.

For the H1N1 strain, site occupancy between the embryo- and MDCK-derived HAs was similar. The first and second glycosylation sites on HAs of H1N1 were on two consecutive

both in the amino acid sequences and on the HA structures. CE, chicken embryo-derived HAs; MDCK, MDCK-derived HAs

Asp residuals. The first potential site was lightly occupied for embryo- and MDCK-derived HAs at 13.1% and 6.74%, respectively, and the second site was partially occupied at 86.9% and 93.3%, respectively. The combined occupancy of the first and second sites was about 100%. All other sites, except the two undetermined sites, were close to fully occupied.

The distribution of the level of site occupancy for all three strains propagated in both chicken embryo and MDCK cells is illustrated in Fig. 2d. The level of occupancy of H1N1 sites was similar between embryo- and MDCK-derived HAs, but embryo-derived H3N2 and B HAs contained more highly glycosylated sites than their MDCK-derived counterparts.

Probability of site occupation predicted by NetNGlyc 1.0 Server (<http://www.cbs.dtu.dk/services/NetNGlyc/>) is included in Table 1. A comparison between the predicted

Table 1 Overview of predicted glycosylation possibility and measured site occupancy of potential glycosylation sites of HAs of (I) X178A (H1N1), (II) NIB-88 (H3N2), and (III) BX-35###(B) derived from both chicken embryo and MDCK propagated vaccines. The results represent the average of three independent measurements

Potential glycosylation site	Amino acid sequence of Asn on HA	Amino acid sequence at the site	Site occupancy (embryo) (% SD)	Site occupancy (MDCK) (% SD)	Predicted occupancy probability
(I)					
#1	10	NNST	13.1 (5.8)	6.7 (4.3)	-
#2	11	NSTD	86.9 (2.6)	93.3 (0.16)	+++
#3	23	NVTV	97.8 (1.4)	99.3 (0.09)	+++
#4	87	NGTC	N.D.	N.D.	+
#5	276	NTTC	98.1 (1.7)	100.0 (0.01)	-
#6	287	NTSL	99.5 (0.23)	100.0 (0.01)	++
#7	481	NGTY	99.0 (0.9)	99.9 (0.04)	+
#8	540	NGSL	N.D.	N.D.	++
(II)					
#1	8	NSTA	98.8 (0.22)	93.5 (0.34)	+++
#2	22	NGTI	99.7 (0.08)	94.5 (0.15)	++
#3	38	NATE	97.5 (0.61)	95.2 (1.3)	+
#4	45	NSSI	40.6 (3.4)	27.8 (5.3)	+
#5	63	NCTL	97.6 (0.09)	98.1 (0.21)	++
#6	122	NESF	18.2 (2.9)	12.2 (5.7)	-
#7	133	NGTS	98.0 (0.25)	99.1 (0.36)	+
#8	144	NSSF	54.8 (3.8)	47.3 (4.1)	+
#9	165	NVTM	99.4 (0.07)	99.6 (0.09)	+++
#10	246	NSTG	94.5 (1.2)	88.2 (1.9)	+
#11	285	NGSI	95.6 (0.33)	95.5 (1.12)	++
#12	483	NGTY	99.5 (0.11)	98.9 (0.08)	+
(III)					
#1	25	NVTG	99.3 (0.02)	97.8 (0.06)	+++
#2	59	NCTD	95.8 (0.39)	87.7 (1.49)	+++
#3	145	NITN	97.8 (0.42)	93.4 (0.64)	+
#4	166	NKTA	96.6 (0.32)	96.9 (3.0)	+
#5	233	NQTE	98.3 (0.03)	96.7 (0.75)	+
#6	304	NKSK	98.9 (0.27)	97.9 (0.05)	+++
#7	333	NGTK	95.9 (1.2)	98.0 (0.73)	+++
#8	492	NQTC	99.0 (0.56)	84.4 (4.1)	-
#9	518	NITA	96.1 (1.7)	97.1 (0.57)	+
#10	531	NHTI	N.D.	N.D.	+
#11	563	NVSC	27.4 (6.8)	65.9 (5.2)	+

N.D., not determined; +++, highly likely; -, not likely

and measured results indicated that the theoretical prediction is not yet fully reliable. For all four sites predicted to be at an extremely low occupancy (#1 and #5 of H1N1, #6 of H3N2, and #8 of B strain), two were indeed low in occupancy (<20%), but the other two had high occupancy at 84.4% to 100% in both chicken embryo-derived and MDCK-derived HAs.

Distribution of glycan structures

PA-labeled glycans were separated by HILIC-HPLC, and the structures of glycans in each peak were elucidated in

subsequent MS/MS analysis. The HILIC-HPLC chromatographs of PA-labeled glycans are shown in Fig. 3a–c. Of all three strains, X179A (H1N1) showed the highest glycan diversity. Glycan structures were determined by GlycoWorkbench based on both the primary and secondary mass spectra. Glycan structures in most HILIC-HPLC peaks are identified and labeled in Fig. 3a–c. Detailed glycan information for all identified glycans is summarized in Table 2. Figure S3 illustrates the procedure in which the structure of glycan in a HILIC-HPLC peak was determined. It should be noted that although there is generally one glycan in each peak, multiple glycans of the same molecular weight may exist in a

single peak, and one glycan could be located in two or three neighboring peaks (Table 2). The abundance (percentage) of each glycan is defined by the ratio of its surface area to the whole surface area in the HILIC-HPLC chromatogram. For a peak that contains more than one glycan, the composition of all glycans in the specific peak were determined by extracted ion chromatograms and express each composition as a % area of all areas from all compositions detected in the fraction pool. As shown in Fig. 3a–c, the longer the retention time in the HILIC-HPLC, the higher the molecular weight of the glycan. For all three strains, there are more high-molecular weight glycans for MDCK-derived HAs than those in embryo-derived HAs. This is more pronounced beyond an elution time of 105 min.

High-mannose structures comprised the most predominant class of glycans for CE and MDCK derived HAs of NIB-88 (H3N2) and BX-35### (B), while for HAs of X179A (H1N1) derived in CE and MDCK, complex and high-mannose glycans were the two equally dominant glycans (Fig. 3d). Of nearly 30 glycans identified, 6 high-mannose glycans, Man5 (Hex5HexNac2) to Man10 (Hex10HexNac2), accounted for 40–60% of all glycans in various samples, as shown in Fig. 3e. For X179A (H1N1), Man8 was the most abundant glycan for both the embryo- and MDCK-derived HAs, while Man9 and Man7 were the most abundant glycan for NIB-88 (H3N2) and BX-35### (B), respectively. The abundance of different glycans between the embryo- and MDCK-derived HAs varied for different strains. For the BX-35### (B) strain, egg embryo-derived HAs had less than 2% Man9, but MDCK-derived HAs had nearly 9% of Man9. A small amount of sulfated glycans was observed on all embryo-derived HAs, but only MDCK-derived HAs of X179A (H1N1) contained sulfated glycans, as shown in Fig. 3f.

Confirmation of high-mannose structures

Enzymatic digestion with Endo H_f and α 1-2,3,6 mannosidase were used to confirm that the high abundance glycans were indeed high-mannose structures. Endo H_f, an endoglycosidase, cleaves within the chitobiose core of high-mannose glycans, and α 1-2,3,6 mannosidase, a broad specificity exoglycosidase, hydrolyzes terminal α 1-2, α 1-3, and α 1-6 linked mannoses. As shown in Fig. 3g and h for embryo- and MDCK derived HAs respectively, Endo H_f and α 1-2,3,6 mannosidase treatment of HAs of NIB-88 (H3N2) eliminated all high-mannose peaks from Man5 (Hex5HexNac2) to Man10 (Hex10HexNac2), as indicated by the star signs. Two new peaks (indicated by triangle signs) corresponding to the remaining fluorescent residuals, PA-GlcNAc and PA-GlcNAc-GlcNAc-Man, were evident after Endo H_f and α 1-2,3,6 mannosidase cleavage respectively. The content of hybrid glycans, defined as those with one

arm of high-mannose structure while the other arm was capped with a galactose, was low. After α 1-2,3,6 mannosidase cleavage, only a slight increase in the corresponding residual was observed, as indicated by the pound sign. Endo H_f and α 1-2,3,6 mannosidase cleavage of the HAs of X179A (H1N1) and BX-35### (B) showed similar results (data not shown). This confirmed that the abundant species on HAs of all three strains were indeed high-mannose structures.

Discussion

MDCK cell cultures have emerged as an important platform for influenza vaccine production (Pérez Rubio and Eiros 2018). It had been reported that glycosylations on HAs produced in MDCK cells were different from that on HAs produced in chicken embryos (Gambaryan et al. 1998; Mochalova et al. 2003), but a systematic comparison of glycosylation on all three strains (H1N1, H3N2, and B) used for trivalent seasonal flu vaccines production was still incomplete. We studied glycosylation on HAs of the three strains recommended for the trivalent seasonal influenza vaccines for the 2015–2016 Northern Hemisphere season. Variations in the site occupancy of potential glycosylation sites and distribution of glycan structures were observed. Most potential glycosylation sites were highly occupied (>95% occupancy). For the H3N2 and B strains, MDCK-derived HAs contained more partially (<95% occupancy) occupied sites than embryo-derived HAs, with 6 and 4 for H3N2 and 3 and 1 for B strain, respectively. For the H1N1 strain, occupancy levels were similar for chicken embryo- and MDCK-derived HAs, each containing two partially occupied sites. There are one, three, and one sites of poor occupancy (<50%) for H1N1, H3N2, and B strains, respectively for both embryo- and MDCK-derived HAs. The three poor occupancy sites on the HAs of H3N2 (site #4, #6, and #8) are of particular significance as these sites are located in the globular head, close to the receptor-binding region. The high occupancy (>90%) sites at 38, 63, 133, 165, 246, 285 and 483 were also detected by An et al. (2015), however, the poor occupancy sites at 45, 122 and 144 were not included in their study. Poor occupancy sites for H1N1 (site #1) and B (site #11) strains were located in the stem region. It should be noted that when spontaneous deamidation of asparagines occurred at the potential glycosylation sites, although at low possibilities, these sites may be counted as being glycosylated. So the occupancy results should be treated with caution as they may contain small contributions from deamidation.

Occupancy on three potential glycosylation sites, including two on the HAs of X179A (H1N1) and one on the HAs of BX-35### (B), could not be determined as their corresponding peptides could not be recovered post-digestion. Interestingly, previous attempts to determine the occupancy at the same two

Table 2 A summary of all PA-labeled N-glycans detected on HAs and their corresponding prevalence. HAs were from X179A (H1N1), NIB-88 (H3N2), and BX35### (B) derived from chicken embryos and MDCK cells. The results represent the average of three independent measurements. *CE*, chicken embryo-derived HAs; *MDCK*, MDCK-derived HAs

<i>m/z</i>	<i>z</i>	Ionization type	Glycan composition (+PA)	X179A (H1N1)			NIB-88 (H3N2)			BX-35### (B)		
				Peak no.	CE (%)	MDCK (%)	Peak no.	CE (%)	MDCK (%)	Peak no.	CE (%)	MDCK (%)
584.7381	2	[M+H+K] ²⁺	Hex3HexNAc2	-	-	-	1	0.22	0.30	1	0.25	0.26
846.7991	2	[M+K+K] ²⁺	S1Hex3HexNAc4	3	0.10	0.32	-	-	-	-	-	-
665.7646	2	[M+H+K] ²⁺	Hex4HexNAc2	4	0.07	0.56	4	0.33	1.13	4,5	0.51	1.22
787.8177	2	[M+H+K] ²⁺	Hex3HexNAc4	-	-	-	6	0.15	-	-	-	-
927.8051	2	[M+K+K] ²⁺	S1Hex4HexNAc4	7	0.16	-	-	-	-	-	-	-
767.3066	2	[M+H+K] ²⁺	Hex4HexNAc3	7	0.22	2.23	7,8	2.11	0.62	7	0.41	0.50
860.8496	2	[M+H+Na] ²⁺	Hex4HexNAc4	-	-	-	7,8	0.90	0.01	-	-	-
746.7945	2	[M+H+K] ²⁺	Hex5HexNAc2	9	5.44	5.19	9	6.92	5.79	9	6.57	8.74
840.3362	2	[M+H+K] ²⁺	FucHex4HexNAc3	9	0.11	0.08	10	1.35	-	10	0.85	-
1029.3461	2	[M+K+K] ²⁺	S1Hex4HexNAc5	9	0.11	-	-	-	-	-	-	-
970.3781	2	[M+H+K] ²⁺	Hex4HexNAc5	-	-	-	-	-	-	10	-	0.31
848.3343	2	[M+H+K] ²⁺	Hex5HexNAc3	10	1.15	0.24	11	0.96	1.53	11	1.24	2.06
941.8758	2	[M+H+K] ²⁺	FucHex4HexNAc4	-	-	-	10	0.33	-	-	-	-
1008.8316	2	[M+K+K] ²⁺	S1Hex5HexNAc4	10	1.35	0.24	11	0.08	-	10,11	3.89	-
1102.3748	2	[M+K+K] ²⁺	S1FucHex4HexNAc5	10	1.47	-	-	-	-	10	1.03	-
868.8487	2	[M+H+K] ²⁺	Hex4HexNAc4	-	-	-	-	-	-	11	0.05	-
921.3649	2	[M+H+K] ²⁺	FucHex5HexNAc3	13	1.64	0.50	-	-	-	13	0.49	0.32
913.3637	2	[M+H+Na] ²⁺	FucHex5HexNAc3	-	-	-	13	1.03	-	13	-	-
1081.8623	2	[M+K+K] ²⁺	S1FucHex5HexNAc4	13	0.67	0.19	13	0.69	-	13	1.53	-
1091.3941	2	[M+H+K] ²⁺	Hex8HexNAc3	-	-	-	-	-	-	13	3.39	-
827.8212	2	[M+H+K] ²⁺	Hex6HexNAc2	14	6.25	5.36	14	7.26	7.59	14	9.98	15.24
949.8752	2	[M+H+K] ²⁺	Hex5HexNAc4	14	1.06	0.61	12	2.22	2.50	14	1.30	2.89
1051.4158	2	[M+H+K] ²⁺	Hex5HexNAc5	15	4.98	3.24	15	4.60	3.65	15	6.39	2.62
1022.9076	2	[M+H+Na] ²⁺	Hex6HexNAc4	16,19	10.05	3.36	16,19	9.12	2.31	16,19	5.31	3.26
929.3617	2	[M+H+K] ²⁺	Hex6HexNAc3	17	1.78	1.83	17	2.96	2.65	17	2.43	2.92
1124.4455	2	[M+H+Na] ²⁺	FucHex5HexNAc5	18	5.71	5.55	18	4.11	1.53	18	5.61	5.57
1030.9008	2	[M+H+K] ²⁺	Hex6HexNAc4	-	-	-	18	0.56	4.96	19	-	3.99
908.8513	2	[M+H+K] ²⁺	Hex7HexNAc2	20	11.05	10.43	20	11.6	11.14	20	22.28	17.70
767.9469	3	[M+H+2K] ³⁺	Hex6HexNAc5	-	-	-	21	0.12	2.45	-	-	-
1095.9372	2	[M+H+Na] ²⁺	FucHex6HexNAc4	21	-	3.72	21,22	5.52	4.77	-	-	-
855.9418	3	[M+3K] ³⁺	FucHex9HexNAc3	21	1.96	-	-	-	-	21	4.13	-
1095.9360	2	[M+H+K] ²⁺	Fuc2Hex5HexNAc4	21	3.64	-	-	-	-	21	2.26	-
1084.9421	2	[M+H+H] ²⁺	FucHex6HexNAc4	-	-	-	-	-	-	21	-	3.14
1002.3946	2	[M+H+K] ²⁺	FucHex6HexNAc3	22	3.31	2.71	-	-	-	21	3.44	-
816.6379	3	[M+H+2K] ³⁺	FucHex6HexNAc5	22	0.58	0.48	-	-	-	-	-	-
1010.3892	2	[M+H+K] ²⁺	Hex7HexNAc3	23	1.28	4.73	23	1.57	1.10	22	1.60	1.47
1197.4763	2	[M+H+K] ²⁺	Fuc2Hex5HexNAc5	23	1.91	-	23	0.84	3.92	22	1.26	-
1186.4818	2	[M+H+H] ²⁺	FucHex6HexNAc5	-	-	-	-	-	-	22	-	3.62
923.6368	3	[M+3K] ³⁺	FucHex9HexNAc4	-	-	-	-	-	-	23	1.78	-
754.2724	3	[M+H+2K] ³⁺	Hex7HexNAc4	-	-	-	25	1.29	0.92	-	-	-
816.6362	3	[M+H+2K] ³⁺	FucHex6HexNAc5	25	3.58	5.87	25	0.92	0.63	-	-	-
1092.9396	2	[M+H+H] ²⁺	Hex7HexNAc4	26	1.89	4.85	-	-	-	26	-	3.76
989.8753	2	[M+H+K] ²⁺	Hex8HexNAc2	27	11.46	11.83	26,27	12.39	11.92	27	8.92	8.07
1184.9583	2	[M+H+K] ²⁺	FucHex7HexNAc4	-	-	-	28	-	1.39	-	-	-
859.9937	3	[M+H+Na+K] ³⁺	Fuc2Hex6HexNAc5	28	1.59	-	-	-	-	-	-	-

Table 2 (continued)

<i>m/z</i>	<i>z</i>	Ionization type	Glycan composition (+PA)	X179A (H1N1)			NIB-88 (H3N2)			BX-35### (B)		
				Peak no.	CE (%)	MDCK (%)	Peak no.	CE (%)	MDCK (%)	Peak no.	CE (%)	MDCK (%)
1083.4219	2	[M+H+K] ²⁺	FucHex7HexNAc3	28	1.60	-	28	1.45	-	-	-	-
870.6544	3	[M+H+2K] ³⁺	FucHex7HexNAc5	29	-	6.85	29	-	3.03	-	-	-
1070.9053	2	[M+H+K] ²⁺	Hex9HexNAc2	30	4.12	6.57	30	15.04	19.37	30	1.39	8.86
938.3482	3	[M+H+2K] ³⁺	FucHex7HexNAc6	31	-	4.32	31	1.37	1.53	31	-	3.04
992.3641	3	[M+H+2K] ³⁺	FucHex8HexNAc6	-	-	-	32	0.07	0.59	-	-	-
924.6724	3	[M+H+2K] ³⁺	FucHex8HexNAc5	-	-	-	32	0.10	0.89	-	-	-
1151.9272	2	[M+H+K] ²⁺	Hex10HexNAc2	32	3.74	3.95	33	1.81	1.79	33	1.71	0.45
1010.3757	3	[M+H+2K] ³⁺	Hex8HexNAc7	34	2.56	2.49	-	-	-	-	-	-
1060.0604	3	[M+H+2K] ³⁺	FucHex8HexNAc7	35	3.42	1.70	-	-	-	-	-	-

Note: 1. -, undetected

2. There were about several ionization types of each N-glycans compositions we have detected, such as [M+H₂]²⁺, [M+H+Na]²⁺, [M+H+K]²⁺, [M+Na+K]²⁺, and [M+K]²⁺ (Figure S3), but we just showed the most abundant ionization type of each N-glycans compositions in Table 2, and all of the ionization types we detected were used in calculation

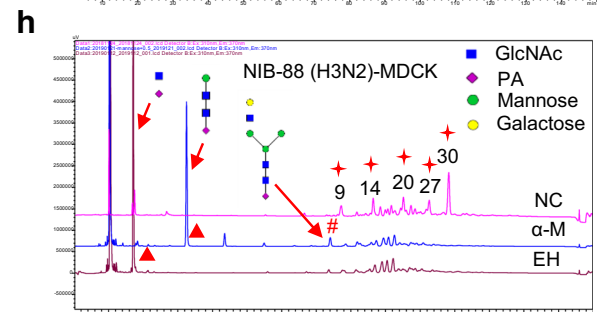
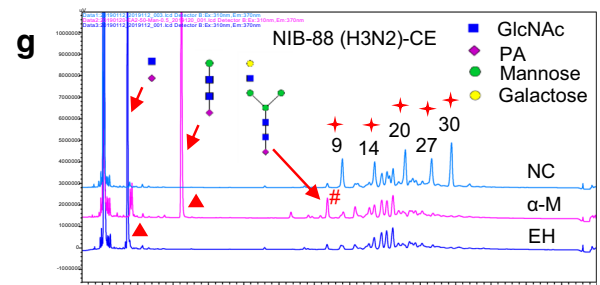
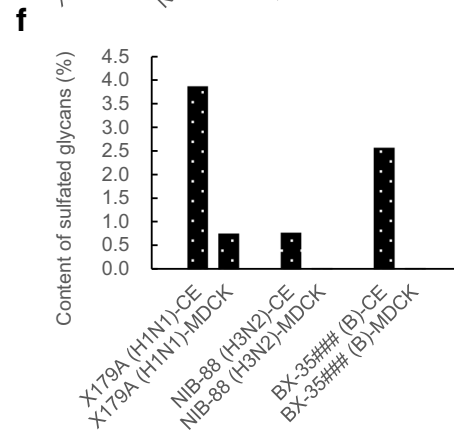
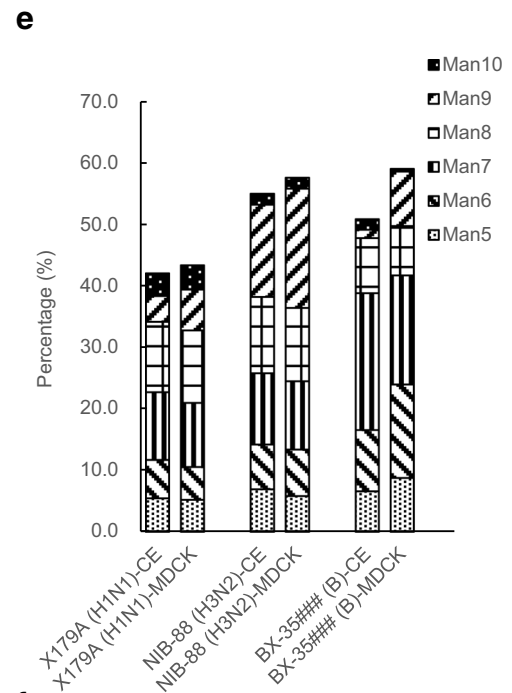
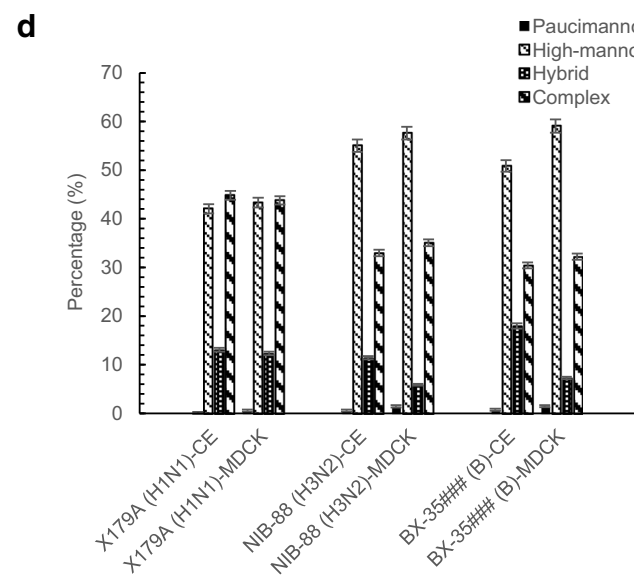
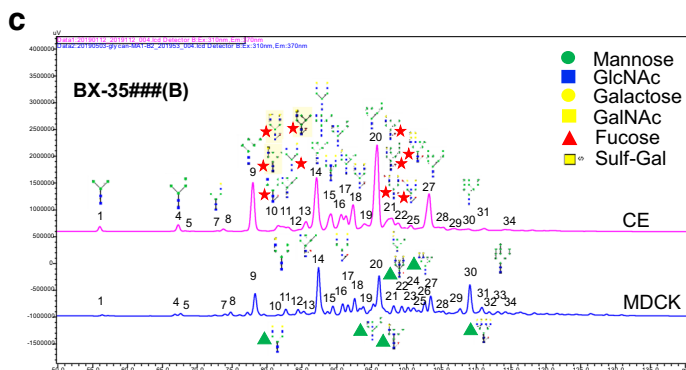
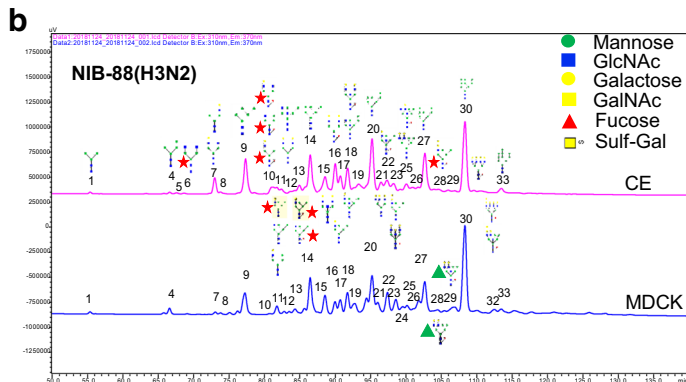
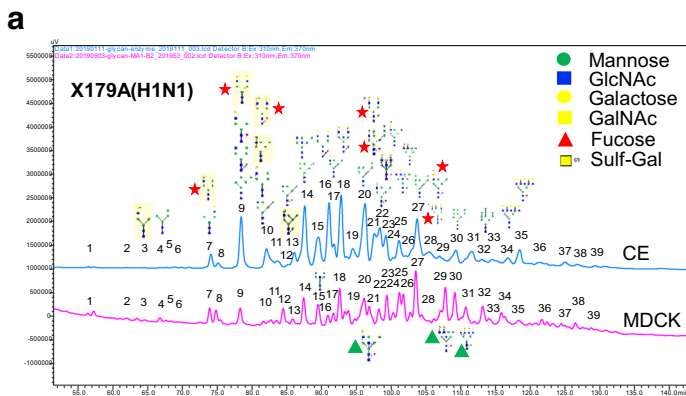
sites on H1N1 HAs were also unsuccessful (Zhang et al. 2012; An et al. 2019). This may require further optimization of the peptide digestion protocol.

The number of glycans on the immunodominant HA head is critical to the fitness of the viruses and the immunogenicity of antigens. Glycans can mask the underlying amino acid epitopes for virus to escape immune pressure. However, the low glycosylation occupancy at #6 and #8 of H3N2 HAs produced in both MDCK cells and embryos may be required for the fitness of the H3N2 strain. The number of glycosylation sites on H3N2 strains increased over time since their introduction into human circulation (Tate et al. 2014). When H3N2 began circulating in humans in 1968, it contained only two glycans in the head region, but the number gradually increased to 6–7 (Tate et al. 2014). The addition of glycans eventually jeopardize the fitness of the viruses as steric hindrance of glycans to RBS reduced avidity of HAs for human receptors and an even lower avidity for avian receptors. In order for circulating H3N2 strains to grow in chicken embryos, they had to be adapted stringently to select mutants with higher affinity to avian receptors. The mutations was suggested to have contributed to the lower effectiveness of H3N2 vaccines (Belongia et al. 2016; Skowronski et al. 2014; Wu et al. 2019). In the 2014–2015 season, a K160T HA mutation brought one more glycosylation site. H3N2 viruses with the K160T mutation grow very poorly in chicken eggs. As a result, H3N2 vaccine strains had to undertake back mutation in order to propagate in eggs, however the immune protection of K160 antigens against circulating H3N2 strain was found to be lower than that of T160 antigens (Zost et al. 2017). Recently, H3N2 seed strains and vaccines without egg adaptation have been isolated and produced in MDCK cells, and a moderate increase in

effectiveness (31.7% vs. 20.1%) was observed (Klein et al. 2020). However, the beneficial effect may be limited to people up to 65 years old (Izurietta et al. 2020; Boikos et al. 2021).

Direct investigations of the impact of glycosylation occupancy on the immunogenicity of HAs are scarce. A recent study by Tseng et al. (2019) reported that monoglycosylated, which contained only a single N-linked GlcNAc and was close to be unglycosylated, H1N1 vaccine elicited higher antibody titers than those elicited by fully glycosylated vaccines. The antibody elicited by monoglycosylated H1N1 HAs showed higher neutralization activity, higher hemagglutination inhibition, and more HA stem selectivity than that fully

Fig. 3 Quantification of different glycans on HAs derived from embryos and MDCK cells (a–c), the content of **d** glycans group, **e** high-mannose glycans, and **f** sulfated glycans, and the shift of the distribution of glycans post-digestion with either **g** α1-2,3,6 mannosidase or **h** Endo Hf. The results in **d**, **e**, and **f** represent the average of three independent measurements. In **d**, error bars represent standard deviation (%). Paucimannose: N-glycans with two HexNAc and less than five Hex. High-mannose: N-glycans with two HexNAc and more than four Hex. Hybrid: N-glycans with three HexNAc. Complex: N-glycans with more than three HexNAc. In **g** and **h**, high-mannose structures were indicated by star signs, residuals of high-mannose structures were indicated by triangle signs, and residuals of hybrid structures were indicated by pound signs. CE, chicken embryo-derived HAs; MDCK, MDCK-derived HAs; GlcNAc, N-acetylglucosamine; GalNAc, N-acetylgalactosamine; Sulf-Gal, sulfated galactose; PA, procainamide; NC, negative control, glycans without enzyme digestion; α-M, α1-2,3,6 mannosidase, glycans with α1-2,3,6 mannosidase digestion; EH, Endo Hf, glycans with Endo Hf digestion. (Fig. 3a–c: The numbers above the peaks represent the corresponding peaks numbers in the chromatogram. The pentagram labeled refers to the glycanform that it is only detected in chicken embryos-derived HA. The triangle labeled refers to the glycanform that it is only detected in MDCK cells-derived HA.)



glycosylated HAs did. However, low coverage of glycans on HAs may expose underlying amino acid epitopes. If the epitopes do not exist in circulating viruses any more, i.e. obsolete epitopes, their exposure may misdirect immune responses in humans.

For H3N2 and B strains, HAs derived from MDCK cells contained more glycans of higher molecular weight than HAs derived from chicken embryos while for the H1N1 strain, glycan profiles were similar between MDCK and embryo derived HAs (Fig. 3d). A higher glycan occupancy and more glycan of higher molecular weight of HAs derived from MDCK cells may explain their seemingly higher molecular weight on SDS-PAGE than those derived from chicken embryos (Fig. 1d and e), but similar molecular weight post deglycosylation (Fig. S4). Similar observation had been reported previously (Romanova et al. 2003).

It has been widely reported that HAs contain a large proportion of high-mannose glycans, although their proportion varies to HAs produced by different hosts. The implication of high-mannose glycans on the effectiveness of influenza vaccines could be complicated. Hütter et al. (2013) found that Vero-derived HAs contained more high-mannose glycans than the MDCK-derived antigens, and Vero-derived HAs were more likely to elicit cellular immunity while MDCK-derived HAs were more likely to elicit humoral immunity. Interestingly, the cellular and humoral immune responses elicited by deglycosylated antigens were significantly reduced, no matter the HAs were derived from Vero or MDCK cells. de Vries et al. (2012) found that recombinant avian H5 HAs produced by insect S2 cells contained more high mannose glycans than those produced by HEK293 cells. HAs with more high-mannose glycans elicited lower antibody titers in chicken and mice than HAs carrying complex glycans. The lower titer was speculated to be associated with either mannose receptor dependent clearance or immunosuppressive activity of terminal mannose on dendritic cells (de Vries et al. 2012). Both β -inhibitors in the serum and surfactant protein-D (SP-D) in the bronchial lavage fluid are innate immune inhibitors that neutralize pathogens through targeting high-mannose glycans (Khatri et al. 2016; Ng et al. 2012). Khatri et al. (2016) found that for a H3N2 HA protein, its affinity to SP-D was significantly higher when two glycosylation sites on the HA head, Asn165 and Asn246, were occupied with high-mannose glycans rather than being eliminated. In addition, An et al. (2019) found that in influenza antigens produced by egg, MDCK cells, or Sf9 cells of different level of high-mannose glycans, single radial immunodiffusion assay (SRID) showed no difference, suggesting more sensitive assays might be required to detect the differences.

High-mannose glycans accounted for 42–57% of all glycans in our studies. The range reported in this study was lower than results reported previously. Yagi et al. (2012) revealed about 30% and 63% of high-mannose glycans on a H3N2

strain derived from egg and MDCK, respectively. But it should be noted that the glycans were released from intact influenza viruses, not from purified HAs. Khatri et al. (2016) reported about 60% high-mannose glycans on HAs of a H3N2 strain produced in eggs. In the analysis of 2014–2015 season influenza vaccine standards, An et al. (2019) reported high-mannose glycans of 63–84% in three strains (H1N1, H3N2, and B) produced in eggs, MDCK cells, or Sf9 cells. The relative low high-mannose glycan content that we observed is mostly like due to the high sensitivity of the assay used this study for which more low-abundance hybrid and complex glycan species were accounted, as seen in Fig. 3d.

The impact of glycosylation on the immunogenic properties of HAs warrants further investigation. At the same time, one of the targets for influenza vaccine is to produce antigenically matched HAs to the circulating strains; therefore, it would be beneficial to analyze glycosylation patterns of HAs in human clinical samples. Site specific glycosylation, especially for the sites around the receptor-binding site, was not investigated in this study. This would be conducted in subsequent investigations.

Supplementary Information The online version contains supplementary material available at <https://doi.org/10.1007/s00253-021-11247-5>.

Code availability Not applicable

Author contribution N. M., Y. Y., and J. L. conceived and designed research. J. L., S. L., Y. G., and S. T. conducted experiments. J. L., S. L., and Y. G. analyzed data. J. L., Y. G., and N. M. wrote the manuscript. All authors read and approved the manuscript.

Funding This work was supported by the Department of Science and Technology of Liaoning Province, China, Project #2014226034.

Data availability The data that support the findings of this study are available from the corresponding author upon reasonable request.

Declarations

Ethics approval This article does not contain any studies with human participants or animals performed by any of the authors.

Consent to participate Not applicable

Consent for publication All authors have read and approved the manuscript for submission and publication.

Conflict of interest The authors declare no competing interests.

References

- Abe Y, Takashita E, Sugawara K, Matsuzaki Y, Muraki Y, Hongo S (2004) Effect of the addition of oligosaccharides on the biological activities and antigenicity of influenza A/H3N2 virus

- hemagglutinin. *J Virol* 78(18):9605–9611. <https://doi.org/10.1128/JVI.78.18.9605-9611.2004>
- Alymova IV, York IA, Air GM, Cipollo JF, Gulati S, Baranovich T, Kumar A, Zeng H, Gansebom S, McCullers JA (2016) Glycosylation changes in the globular head of H3N2 influenza hemagglutinin modulate receptor binding without affecting virus virulence. *Sci Rep* 6:36216. <https://doi.org/10.1038/srep36216>
- An Y, McCullers JA, Alymova I, Parsons LM, Cipollo JF (2015) Glycosylation analysis of engineered H3N2 influenza A virus hemagglutinins with sequentially added historically relevant glycosylation sites. *J Proteome Res* 14(9):3957–3969. <https://doi.org/10.1021/acs.jproteome.5b00416>
- An Y, Parsons LM, Jankowska E, Melnyk D, Joshi M, Cipollo JF (2019) N-glycosylation of seasonal influenza vaccine hemagglutinins: implication for potency testing and immune processing. *J Virol* 93(2). <https://doi.org/10.1128/JVI.01693-18>
- Belongia EA, Simpson MD, King JP, Sundaram ME, Kelley NS, Osterholm MT, McLean HQ (2016) Variable influenza vaccine effectiveness by subtype: a systematic review and meta-analysis of test-negative design studies. *Lancet Infect Dis* 16:942–951. [https://doi.org/10.1016/S1473-3099\(16\)00129-8](https://doi.org/10.1016/S1473-3099(16)00129-8)
- Blackburne BP, Hay AJ, Goldstein RA (2008) Changing selective pressure during antigenic changes in human influenza H3. *PLoS Pathog* 4(5):e1000058. <https://doi.org/10.1371/journal.ppat.1000058>
- Boikos C, Fischer L, O'Brien D, Vasey J, Sylvester GC, Mansi JA (2021) Relative effectiveness of the cell-derived inactivated quadrivalent influenza vaccine versus egg-derived inactivated quadrivalent influenza vaccines in preventing influenza-related medical encounters during the 2018–2019 influenza season in the United States. *Clin Infect Dis*. <https://doi.org/10.1093/cid/ciaa1944>
- Cherry JL, Lipman DJ, Nikolskaya A, Wolf YI (2009) Evolutionary dynamics of N-glycosylation sites of influenza virus hemagglutinin. *PLoS Curr* 1:RRN1001. <https://doi.org/10.1371/currents.RRN1001>
- Daniels R, Kurowski B, Johnson AE, Hebert DN (2003) N-linked glycans direct the cotranslational folding pathway of influenza hemagglutinin. *Mol Cell* 11(1):79–90. [https://doi.org/10.1016/S1097-2765\(02\)00821-3](https://doi.org/10.1016/S1097-2765(02)00821-3)
- Das SR, Hensley SE, David A, Schmidt L, Gibbs JS, Puigbò P, Ince WL, Bennis JR, Yewdell JW (2011) Fitness costs limit influenza A virus hemagglutinin glycosylation as an immune evasion strategy. *Proc Natl Acad Sci* 108(51):20289–20290. <https://doi.org/10.2307/23077234>
- Dreyfus C, Laursen NS, Kwaks T, Zuijdgheest D, Khayat R, Ekiert DC, Lee JH, Metlagel Z, Jongeneelen M, Vlugt RVD, Lamrani M, Korse HJWM, Geelen E, Sahin Ö, Siewwert M, Brakenhoff JPI, Vogels R, Li OTW, Poon LLM, Peiris M, Koudstaal W, Ward AB, Wilson IA, Goudsmit J, Friesen RHE (2012) Highly conserved protective epitopes on influenza B viruses. *Science* 337(6100):1343–1348. <https://doi.org/10.1126/science.1222908>
- Gallagher PJ, Henneberry JM, Sambrook JF, Gething MJ (1992) Glycosylation requirements for intracellular transport and function of the hemagglutinin of influenza virus. *J Virol* 66(12):7136–7145. [https://doi.org/10.1016/0166-0934\(92\)90092-R](https://doi.org/10.1016/0166-0934(92)90092-R)
- Gambaryan AS, Marinina VP, Tuzikov AB, Bovin NV, Rudneva IA, Sinityn BV, Shilov BV, Matrosovich MN (1998) Effects of host-dependent glycosylation of hemagglutinin on receptor-binding properties of H1N1 human influenza A virus grown in MDCK cells and in embryonated eggs. *Virology* 247(2):170–177. <https://doi.org/10.1042/BJ20112101>
- Gerdil C (2003) The annual production cycle for influenza vaccine. *Vaccine* 21(16):1776–1779. [https://doi.org/10.1016/S0264-410X\(03\)00071-9](https://doi.org/10.1016/S0264-410X(03)00071-9)
- Hebert DN, Zhang JX, Chen W, Foellmer B, Helenius A (1997) The number and location of glycans on influenza hemagglutinin determine folding and association with calnexin and calreticulin. *J Cell Biol* 139(3):613–623. <https://doi.org/10.1083/jcb.139.3.613>
- Hütter J, Rödiger JV, Höper D, Seeberger PH, Reichl U, Rapp E, Lepenies B (2013) Toward animal cell culture-based influenza vaccine design: viral hemagglutinin N-glycosylation markedly impacts immunogenicity. *J Immunol* 190(1):220–230. <https://doi.org/10.4049/jimmunol.1201060>
- Izurrieta HS, Chillarige Y, Kelman J, Wei Y, Lu Y, Xu W, Lu M, Pratt D, Wernecke M, Macurdy T, Forshee R (2020) Relative effectiveness of influenza vaccines among the United States elderly, 2018–2019. *J Infect Dis* 222(2):278–287. <https://doi.org/10.1093/infdis/jiaa080>
- Kaiser J (2006) A one-size-fits-all flu vaccine? *Science* 312(5772):380–382. <https://doi.org/10.1126/science.312.5772.380>
- Khatri K, Klein JA, White MR, Grant OC, Leymarie N, Woods RJ, Hartshorn KL, Zaia J (2016) Integrated omics and computational glycobiology reveal structural basis for influenza A virus glycan microheterogeneity and host interactions. *Mol Cell Proteomics* 15(6):1895–1912. <https://doi.org/10.1074/mcp.M116.058016>
- Klein NP, Fireman B, Goddard K, Zerbo O, Asher J, Zhou J, King J, Lewis N (2020) Vaccine effectiveness of cell-culture relative to egg-based inactivated influenza vaccine during the 2017–18 influenza season. *PLoS One* 15(2):e0229279. <https://doi.org/10.1371/journal.pone.0229279>
- Kobayashi Y, Suzuki Y (2012) Evidence for N-glycan shielding of antigenic sites during evolution of human influenza A virus hemagglutinin. *J Virol* 86(7):3446–3451. <https://doi.org/10.1128/JVI.06147-11>
- Lee PS, Ohshima N, Stanfield RL, Yu W, Iba Y, Okuno Y, Kurosawa Y, Wilson IA (2014) Receptor mimicry by antibody F045–092 facilitates universal binding to the H3 subtype of influenza virus. *Nat Commun* 5(1):1–9. <https://doi.org/10.1038/ncomms4614>
- Matrosovich M, Zhou N, Kawaoka Y, Webster R (1999) The surface glycoproteins of h5 influenza viruses isolated from humans, chickens, and wild aquatic birds have distinguishable properties. *Virology* 73:1146–1155. <https://doi.org/10.1128/JVI.73.2.1146-1155.1999>
- Medina RA, Stertz S, Manicassamy B, Zimmermann P, Sun X, Albrecht RA, Kerttula HU, Zagordi O, Belshe RB, Frey SE, Tumpey TM, Sastre AG (2013) Glycosylations in the globular head of the hemagglutinin protein modulate the virulence and antigenic properties of the H1N1 influenza viruses. *Sci Transl Med* 5(187):187ra70. <https://doi.org/10.1126/scitranslmed.3005996>
- Mochalova L, Gambaryan A, Romanova J, Tuzikov A, Chinarev A, Katinger D, Katinger H, Egorov A, Bovin N (2003) Receptor-binding properties of modern human influenza viruses primarily isolated in Vero and MDCK cells and chicken embryonated eggs. *Virology* 313(2):473–480. [https://doi.org/10.1016/s0042-6822\(03\)00377-5](https://doi.org/10.1016/s0042-6822(03)00377-5)
- Ng WC, Tate MD, Brooks AG, Reading PC (2012) Soluble host defense lectins in innate immunity to influenza virus. *J Biomed Biotechnol* 2012:732191. <https://doi.org/10.1155/2012/732191>
- Ohuchi M, Ohuchi R, Feldmann A, Klenk HD (1997) Regulation of receptor binding affinity of influenza virus hemagglutinin by its carbohydrate moiety. *Virology* 71:8377–8384. <https://doi.org/10.1128/JVI.71.11.8377-8384.1997>
- Pérez Rubio A, Eiros JM (2018) Cell culture-derived flu vaccine: Present and future. *Hum Vacc Immunother* 14(8):1874–1882. <https://doi.org/10.1080/21645515.2018.1460297>
- Roberts PC, Garten W, Klenk HD (1993) Role of conserved glycosylation sites in maturation and transport of influenza A virus hemagglutinin. *J Virol* 67(6):3048–3060. <https://doi.org/10.1620/tjem.106.83>
- Rockman S, Laurie KL, Parkes S, Wheatley A, Barr IG (2020) New technologies for influenza vaccines. *Microorganisms* 8(11):1745. <https://doi.org/10.3390/microorganisms8111745>
- Romanova J, Katinger D, Ferko B, Voglauer R, Mochalova L, Bovin N, Lim W, Katinger H, Egorov A (2003) Distinct host range of influenza H3N2 virus isolates in Vero and MDCK cells is determined by

- cell specific glycosylation pattern. *Virology* 307(1):90–97. [https://doi.org/10.1016/S0042-6822\(02\)00064-8](https://doi.org/10.1016/S0042-6822(02)00064-8)
- Schwarzer J, Rapp E, Hennig R, Genzel Y, Jordan I, Sandig V, Reichl U (2009) Glycan analysis in cell culture-based influenza vaccine production: influence of host cell line and virus strain on the glycosylation pattern of viral hemagglutinin. *Vaccine* 27(32):4325–4336. <https://doi.org/10.1016/j.vaccine.2009.04.076>
- Skehel JJ, Stevens DJ, Daniels RS, Douglas AR, Knossow M, Wilson IA, Wiley DC (1984) A carbohydrate side chain on hemagglutinins of Hong Kong influenza viruses inhibits recognition by a monoclonal antibody. *Proc Natl Acad Sci* 81(6):1779–1783. <https://doi.org/10.1073/pnas.81.6.1779>
- Skowronski DM, Janjua NZ, De Serres G, Sabaiduc S, Eshaghi A, Dickinson JA, Fonseca K, Winter AL, Gubbay JB, Krajden M, Petric M, Charest H, Bastien N, Kwindt TL, Mahmud SM, Caesele PV, Li Y (2014) Low 2012–13 influenza vaccine effectiveness associated with mutation in the egg-adapted H3N2 vaccine strain not antigenic drift in circulating viruses. *PLoS One* 9:e92153. <https://doi.org/10.1371/journal.pone.0092153>
- Sun S, Wang Q, Zhao F, Chen W, Li Z (2011) Glycosylation site alteration in the evolution of influenza A (H1N1) viruses. *PLoS One* 6(7):e22844. <https://doi.org/10.1371/journal.pone.0022844>
- Tate MD, Job ER, Deng YM, Gunalan V, Maurer-Stroh S, Reading PC (2014) Playing hide and seek: how glycosylation of the influenza virus hemagglutinin can modulate the immune response to infection. *Viruses* 6(3):1294–1316. <https://doi.org/10.3390/v6031294>
- Tseng YC, Wu CY, Liu ML, Chen TH, Chiang WL, Yu YH, Jan JT, Lin KI, Wong CH, Ma C (2019) Egg-based influenza split virus vaccine with monoglycosylation induces cross-strain protection against influenza virus infections. *Proc Natl Acad Sci U S A* 116(10):4200–4205. <https://doi.org/10.1073/pnas.1819197116>
- de Vries RP, Smit CH, de Bruin E, Rigter A, de Vries E, Cornelissen LA, Eggink D, Chung NP, Moore JP, Sanders RW, Hokke CH, Koopmans M, Rottier PJ, de Haan CA (2012) Glycan-dependent immunogenicity of recombinant soluble trimeric hemagglutinin. *J Virol* 86(21):11735–11744. <https://doi.org/10.1128/JVI.01084-12>
- Wang W, Lu B, Zhou H, Suguitan AL, Cheng X, Subbarao K, Kemple G, Jin H (2010) Glycosylation at 158n of the hemagglutinin protein and receptor binding specificity synergistically affect the antigenicity and immunogenicity of a live attenuated H5N1 a/vietnam/1203/2004 vaccine virus in ferrets. *Virol* 84:6570–6577. <https://doi.org/10.1128/JVI.00221-10>
- Wei CJ, Boyington JC, Dai K, Houser KV, Pearce MB, Kong WP, Yang ZY, Tumpey TM, Nabel GJ (2010) Cross-neutralization of 1918 and 2009 influenza viruses: role of glycans in viral evolution and vaccine design. *Sci Transl Med* 2(24):24ra21. <https://doi.org/10.1126/scitranslmed.3000799>
- Wrigley NG, Brown EB, Daniels RS, Douglas AR, Skehel JJ, Wiley DC (1983) Electron microscopy of influenza haemagglutinin-mono-clonal antibody complexes. *Virology* 131(2):308–314. [https://doi.org/10.1016/0042-6822\(83\)90499-3](https://doi.org/10.1016/0042-6822(83)90499-3)
- Wu NC, Lv H, Thompson AJ, Wu DC, Ng WW, Kadam RU, Lin C, Nycholat CM, McBride R, Liang W, Paulson JC, Mok CKP, Wilson IA (2019) Preventing an antigenically disruptive mutation in egg-based H3N2 seasonal influenza vaccines by mutational incompatibility. *Cell Host Microbe* 25(6):836–844. <https://doi.org/10.1016/j.chom.2019.04.013>
- Yagi H, Watanabe S, Suzuki T, Takahashi T, Suzuki Y, Kato K (2012) Comparative analyses of N-glycosylation profiles of influenza A viruses grown in different host cells. *Open Glycosci* 5:2–12. <https://doi.org/10.2174/1875398101205010002>
- Zhang M, Gaschen B, Blay W, Foley B, Haigwood N, Kuiken C, Korber B (2004) Tracking global patterns of N-linked glycosylation site variation in highly variable viral glycoproteins: HIV, SIV, and HCV envelopes and influenza hemagglutinin. *Glycobiology* 14(12):1229–1246. <https://doi.org/10.1093/glycob/cwh106>
- Zhang W, Qi J, Shi Y, Li Q, Gao F, Sun Y, Lu X, Lu Q, Vavricka CJ, Liu D, Yan JH, Gao GF (2010) Crystal structure of the swine-origin A (H1N1)-2009 influenza A virus hemagglutinin (HA) reveals similar antigenicity to that of the 1918 pandemic virus. *Protein Cell* 1(5):459–467. <https://doi.org/10.1007/s13238-010-0059-1>
- Zhang S, Sherwood RW, Yang Y, Fish T, Chen W, McCardle JA, Jones RM, Yusibov V, May ER, Rose JKC, Thannhauser TW (2012) Comparative characterization of the glycosylation profiles of an influenza hemagglutinin produced in plant and insect hosts. *Proteomics* 12(8):1269–1288. <https://doi.org/10.1002/pmic.201100474>
- Zost SJ, Parkhouse K, Gumina ME, Kim K, Perez SD, Wilson PC, Treanor JJ, Sant AJ, Cobey S, Hensley SE (2017) Contemporary H3N2 influenza viruses have a glycosylation site that alters binding of antibodies elicited by egg-adapted vaccine strains. *Proc Natl Acad Sci U S A* 114(47):12578–12583. <https://doi.org/10.1073/pnas.1712377114>

Publisher's note Springer Nature remains neutral with regard to jurisdictional claims in published maps and institutional affiliations.